

THE EFFECT OF POWER ALLOCATION ON VISIBLE LIGHT COMMUNICATION USING COMMERCIAL PHOSPHOR-CONVERTED LED LAMP FOR INDIRECT ILLUMINATION

Alexis A. Dowhuszko¹, Mehmet Ilter², Paulo Pinho² and Jyri Hämäläinen²

¹Centre Tecnològic de Telecomunicacions de Catalunya (CTTC/CERCA), Castelldefels, Spain

²School of Electrical Engineering (ELEC), Aalto University, Espoo, Finland

Email: alexis.dowhuszko@cttc.es; {mehmet.ilter; paulo.pinho; jyri.hamalainen}@aalto.fi

ABSTRACT

Visible light communication (VLC) systems should be designed to provide illumination and wireless data services simultaneously. To achieve this goal at a *reasonable* cost, the use of Phosphor-Converted (PC) LEDs for indirect illumination should be favored to provide a homogeneous and reliable coverage in the whole service area. Unfortunately, PC-LEDs found in the market so far have not been designed for data transmission; moreover, the response of the other (electro-) optical components of the VLC link are far from *ideal*. In this paper, we estimate the data rate that is feasible with VLC when indirect illumination is used. For this purpose, the end-to-end response of the VLC link is first modeled using actual measurements of the spectral power distribution of a PC-LED lamp and the ceiling reflectance. Then, different power allocation schemes are studied assuming an optical OFDM waveform. As commercial LEDs have a relatively slow time response, the equivalent VLC channel that results has strong frequency selectivity; therefore, notable data rate gains are achievable when waterfilling power allocation is applied.

Index Terms— Visible Light Communication, Illumination, PC-LEDs, Optical OFDM, Power Allocation.

1. INTRODUCTION

Visible Light Communication (VLC) systems using Phosphor-Converted (PC) Light Emitting Diodes (LED) have been considered as an attractive alternative to Radio Frequency (RF) technologies for indoor short-range communications [1]. PC-LEDs offer the cheapest lighting among LED technologies found in the market, providing an optical spectrum that the human eye interprets as a white light source by combining blue and yellow light. Specifically, the PC-LED chip emitting blue light is covered by a phosphorescent layer, such that yellow light is produced from a part of emitted blue light [2].

Most indoor VLC applications found in the literature consider Line-of-Sight (LOS) propagation, where the LEDs are

generally placed on the ceiling to provide a direct illumination towards upward-facing Photodetectors (PDs) located in beneath [3, 4]. However, such an approach might cause non-homogeneous illumination in the service area, discomfort glare effect, and over-exposure problems in light-directed areas [5]. From this perspective, there are only few experimental demonstrations for Non-Line-of-Sight (NLOS) VLC application [6, 7]. However, these publications do not address in detail the data rate that is feasible when the VLC system should also verify given illumination constraints.

DC-biased Optical (DCO)-OFDM, which generates a real *unipolar* baseband signal forcing the Hermitian symmetry condition in the vector of QAM-symbols that feeds the IFFT, plus adding a DC-level and clipping the negative values, is widely employed to mitigate the impact of the low-pass frequency response of the VLC link [8]. In this context, the choice of power allocation strategy also plays an important role, as most references assume a flat (electrical) frequency-response when estimating the achievable data rate [9, 10].

In this paper, the data rate of a VLC system using a PC-LED lamp with indirect illumination is studied assuming different power allocation schemes. In contrast to existing works, real measurements of the PC-LED spectral power distribution and the spectral reflectance of the ceiling material are utilized to obtain more realistic estimations. The data rate that is feasible with indirect illumination has also been characterized for different DCO-OFDM signal bandwidth and power allocation strategies, while fulfilling the illumination requirements that exist for indoor office environments.

2. SYSTEM MODEL

Consider the VLC system model presented in Fig. 1, consisting of a floor lamp with a PC-LED in the center of the room, a ceiling reflecting surface with known spectral reflectance, and a PD on top of a desk. For simplicity, only the downlink direction of communication is considered. Moreover, all signal processing is implemented in transmission, where the QAM symbols are mapped on the different subcarriers of the Optical OFDM signal. In order to model the end-to-end response of the VLC link, the three main blocks of it (*i.e.*, transmitter, channel and receiver) are now described in detail.

This work received funding from the Ministry of Science, Innovation, and Universities of Spain under Project TERESA-TEC2017-90093-C3-1-R (AEI/FEDER, UE), the Catalan government under grant 2017-SGR-01479, and the ATTRACT project funded by the EC under Grant Agreement 777222.

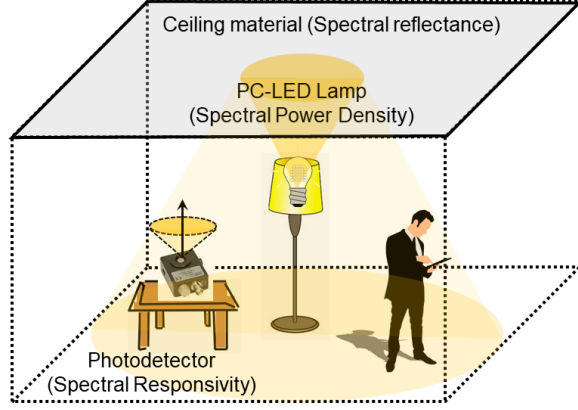


Fig. 1. Indoor VLC system using a floor lamp to provide optical wireless access in presence of indirect illumination.

2.1. VLC transmitter using PC-LEDs

PC-LEDs consist of a blue chip and yellow phosphor layer, whose interaction generates white light. The Correlated Color Temperature (CCT) of the white light that the PC-LED emits depends on the balance between the power of the blue light from the Blue (B)-Chip and the green-yellow-red light converted from the Yellow (Y)-Phosphor layer.

2.1.1. Spectral Power Distribution of PC-LEDs

The data sheets of LEDs originally designed for illumination, such as [11], only provide low-quality plots of the relative Spectral Power Distribution (SPD) of the LED, *i.e.*,

$$G_{\text{rel}}(\lambda) = \frac{S_o^{(w)}(\lambda)}{\max_{\lambda} \{S_o^{(w)}(\lambda)\}}, S_o^{(w)}(\lambda) = S_o^{(b)}(\lambda) + S_o^{(p)}(\lambda), \quad (1)$$

where $S_o^{(b)}(\lambda)$ and $S_o^{(p)}(\lambda)$ are the SPD of the light emitted by the B-Chip and Y-Phosphor, respectively. To characterize the contribution of each of these sources *separately*, given actual measurements of the SPD of the aggregate white light that the PC-LED emits (Cyan solid line in Fig. 2), we apply the curve fitting model proposed in [12] to obtain

$$S_o^{(b)}(\lambda) \approx A_1 \exp \left\{ - \left(\frac{\lambda - \mu_1}{\sigma_1} \right)^2 \right\}, \quad (2)$$

$$S_o^{(p)}(\lambda) \approx A_2 \exp \left\{ - \left(\frac{\lambda - \mu_2}{\sigma_2 [1 + \text{sign}(\lambda - \mu_2) \alpha]} \right)^2 \right\}, \quad (3)$$

where A_1 (A_2) is proportional to optical intensity radiated by the B-chip (Y-phosphor) at the peak wavelength μ_1 (μ_2), σ_1 (σ_2) is proportional to the Full Width at Half Maximum (FWHM) optical power emitted by the B-Chip (Y-phosphor), α indicates the shape of the asymmetric Gaussian function, and $\text{sign}(x)$ is the signum function of real number x that equals 1 for $x \geq 0$ and -1 otherwise.

The parameters that minimize the mean square error between the actual measurement (Solid cyan line) and the curve

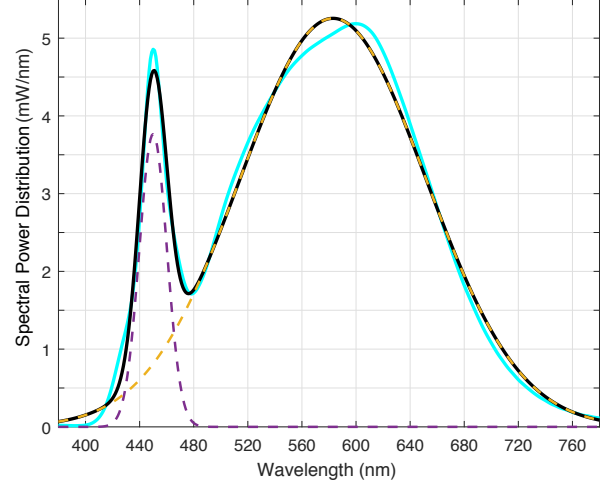


Fig. 2. Measured SPD of neutral white LED light (solid cyan line), and estimated SPD of light emitted by the B-Chip (dashed violet line), Y-Phosphor (dashed yellow line), and the combination of both of them (solid black line).

Table 1. Curve fitting parameters LUXEON Rebel (4000 K).

	Intensity [mW]	Peak λ [nm]	Std. Dev. [nm]
B-Chip	$A_1 = 3.7880$	$\mu_1 = 450$	$\sigma_1 = 14.41$
Y-Phos.	$A_2 = 5.2833$	$\mu_2 = 583$	$\sigma_2 = 97.29$

fitting approximation (Solid black line) for the LUXEON Rebel Plus LX18-P140-3 (4000 K) [11] are listed in Table 1. Note that the area of the curve has been normalized (1 W), and that best fitting takes place when $\alpha \approx 0$. Small discrepancies between data sheet values and actual measurements are due to LED junction temperature variation during the experiment.

2.1.2. Modulation behavior of PC-LEDs

In a PC-LED, two colors are added to produce light that is perceived as white. Due to that, the modulation process with these LEDs can be described as follows [2]: The electrical current that drives the LED (i_{led}) passes through the B-Chip. Then, part of the blue light that the LED chip generates is radiated directly, whereas the remaining part of the emission is first absorbed by the phosphor layer and then spontaneously irradiated at a longer wavelength. The response to the impulse of both B-Chip and Y-Phosphor components can be characterized by two exponential decaying functions, namely

$$h_b(t) = u(t) \exp(-t/\tau_b), \quad h_p(t) = u(t) \exp(-t/\tau_p), \quad (4)$$

where $u(t)$ is the unit step function and τ_b (τ_p) is the time constant for the B-Chip (Y-Phosphor).

The instantaneous optical power of the LED is given by

$$p_{o,\text{tx}}^{(w)}(t) \propto i_{\text{led}} * \left[G_b h_b(t) + G_p h_b(t) * h_p(t) \right], \quad (5)$$

where G_b and G_p are the power gain coefficients that take into account the fraction of the optical power that is received from

the B-Chip and Y-Phosphor, respectively, whereas ‘*’ denotes the convolution operation. Then, the frequency response can be obtained by using the Fourier transform, *i.e.*,

$$H_w(f) = \left[\frac{1}{1 + j2\pi f\tau_b} \right] \left[G_b + G_p \frac{1}{1 + j2\pi f\tau_p} \right]. \quad (6)$$

The time constants τ_b and τ_p are not easy to measure in practice; therefore, we use the values reported in [2].

2.2. Optical wireless channel with ceiling reflection

The optical power that the PD receives in case of indirect illumination depends on the SPD of the LED $S_o^{(w)}(\lambda)$ and the reflectance of the ceiling material $\rho_{\text{ceil}}(\lambda)$. Both of them were measured experimentally to obtain the simulation results.

Based on [13], the DC gain of the optical channel between LED and PD after the first-order reflection on the ceiling is

$$H_{\text{led,pd}}^{\text{indir}}(0) = \sum_i H_{\text{led,i}}^{\text{dir}}(0) H_{\text{i,pd}}^{\text{dir}}(0), \quad (7)$$

where i is the index of each of the (small) non-overlapping reflecting elements in which the ceiling area is divided, and

$$H_{\text{led,i}}^{\text{dir}}(0) = [A_{\text{ref}} \cos^m(\phi_1) \cos(\psi_1)] / [2\pi d_1^2], \quad (8)$$

$$H_{\text{i,pd}}^{\text{dir}}(0) = [A_{\text{pd}} \cos(\phi_2) \cos(\psi_2)] / [\pi d_2^2] \quad \psi_2 \leq \Psi_c, \quad (9)$$

are the DC gain of the direct link between the LED and reflecting element i , and between the reflecting element i and PD, respectively. In (8)-(9), m is the Lambert index of the LED, A_{ref} (A_{pd}) [m^2] is the physical area of the i -th reflecting element (PD), ϕ_1 (ϕ_2) and ψ_1 (ψ_2) [rad] are the angle of irradiance and incidence of the first (second) link, respectively, d_1 (d_2) [m] is the LED-reflector (reflector-PD) distance, and Ψ_c [rad] is the Field of View (FOV) semi-angle of the PD. In practice, the Lambert index $m = -1 / \log_2[\cos(\theta_{\text{max}})]$, where θ_{max} [rad] is the LED radiation semi-angle at half power, which is typically provided by the LED data sheets [11].

Finally, the spectral optical power that reaches the PD is

$$p_{\text{o,pd}}^{(w)}(\lambda) = P_{\text{led}} S_o^{(w)}(\lambda) \rho_{\text{ceil}}(\lambda) H_{\text{led,pd}}^{\text{indir}}(0), \quad (10)$$

where P_{led} [W] is the total radiant power of the LED. The reflectance $\rho_{\text{ceil}}(\lambda)$ that was measured for the white-painted sample ceiling material is shown in Fig. 3 (solid blue line).

2.3. VLC receiver using commercial PD

The DC current at the output of the PD is given by

$$i_{\text{rx}}(0) = \int_{\lambda_l}^{\lambda_u} p_{\text{o,pd}}^{(w)}(\lambda) R_{\text{pd}}(\lambda) f_o(\lambda) d\lambda, \quad (11)$$

where $R_{\text{pd}}(\lambda)$ [A/W] is the responsivity of the PD and $f_o(\lambda)$ is the transmittance of the optical filter with lower (λ_l) and upper (λ_u) cutoff wavelengths. The responsivity of the PD (solid red line) and the transmittance of the optical filter (dashed

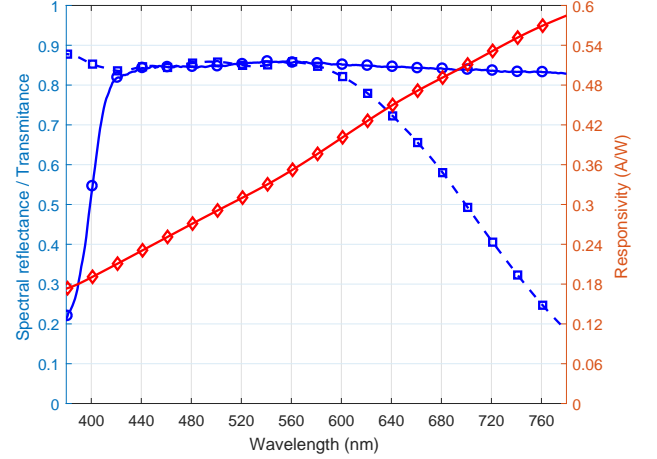


Fig. 3. Measured spectral reflectance of white ceiling material (solid blue), FGS900 visible light filter transmittance (dashed blue), and PDA100A2 PD responsivity (solid red).

blue line) can be appreciated in Fig. 3, and have been taken from the data sheets of PDA100A2 [14] and FGS900 [15] respectively, both of them manufactured by Thorlabs.

Finally, the SNR of the signal at the PD output is given by

$$\Gamma_{\text{pd}}(f) = \Gamma_{\text{pd}}(0) |H_w(f)|^2, \quad \Gamma_{\text{pd}}(0) = \left| \frac{i_{\text{rx}}(0) G_{\text{tia}}}{v_n} \right|^2, \quad (12)$$

where G_{tia} [V/A] is the gain of the Transimpedance Amplifier (TIA) that is placed at the output of the PD, and v_n is the RMS of the aggregate noise that is present at the TIA output.

3. KEY PERFORMANCE INDICATORS FOR VLC

In this paper, two Key Performance Indicators are defined, namely: Illuminance and Achievable Data Rate.

3.1. Illuminance requirements to be verified

Taking into account the human eye sensitivity function $V(\lambda)$, the luminous flux and the illuminance [16] on the PD becomes

$$\Phi = 683 \left[\frac{\text{lm}}{\text{W}} \right] \int_{380\text{nm}}^{780\text{nm}} p_{\text{o,pd}}^{(w)}(\lambda) V(\lambda) d\lambda, \quad E_v = \frac{\Phi}{A_{\text{pd}}}, \quad (13)$$

respectively. When a typical office environment is considered, the mean illuminance $E_{\text{avg}} = E\{E_v\} \geq 500$ [Lux] and the illuminance uniformity $U = \min\{E_v\} / E_{\text{avg}} \geq 0.6$ should be simultaneously verified according to [17].

3.2. Achievable data rate of the VLC link

When DCO-OFDM is utilized, the DC-level γ_{dc} to be added before clipping the negative values of the real baseband OFDM signal should be high enough to do not affect the BER floor of the Adaptive Modulation and Coding (AMC) scheme on each subcarrier. In this situation, the achievable data rate of the VLC link with DCO-OFDM can be written as

$$R_{\text{pa}} = \int_0^W \log_2 \left(1 + \frac{g_{\text{pa}}(f) \Gamma_{\text{pd}}(f)}{\gamma_{\text{dc}}} \right) df, \quad (14)$$

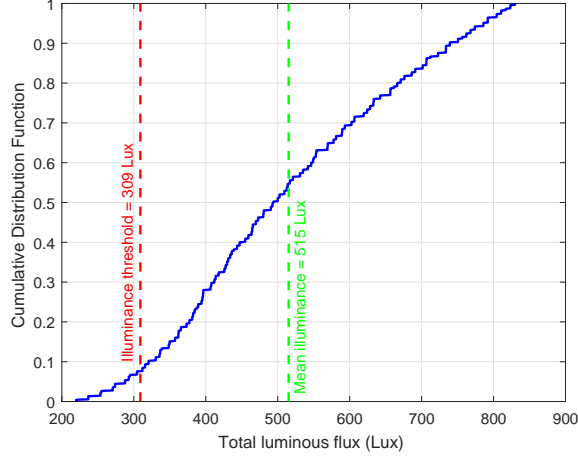


Fig. 4. Cumulative distribution function (CDF) of room illuminance. Red dashed line: Minimum illuminance threshold (60% of mean value). Green dashed line: Mean illuminance.

where W [Hz] is the (one-sided) DCO-OFDM signal bandwidth, whereas $g_{pa}(f)$ depends on the power allocation strategy that is used and verifies $\int_0^W g_{pa}(f) df = W$. Three different power allocation strategies were considered, namely:

- **Equal Power Allocation (EPA):** Assumes that power is evenly divided among the QAM symbols of the different DCO-OFDM subcarriers, such that $g_{pa}(f) = 1$ for $0 \leq f \leq W$. This way, all the electrical bandwidth of the PC-LED is utilized, and the spectral efficiency of the AMC scheme decreases with the indexes of the subcarriers.
- **Equal SNR in Reception (ESNR):** Assumes that the power is unevenly allocated, verifying $g_{pa}(f)\Gamma_{pd}(f) = \Gamma_{esnr}$ for $0 \leq f \leq W$, such that Γ_{esnr} is observed in all subcarriers to achieve the target BER with the same AMC scheme.
- **Waterfilling (WF) Power Allocation:** As expected, the achievable data rate of the VLC link is maximized when $g_{wf}(f) = \max\{0, 1/\nu - \alpha(f)\}$, where $\alpha(f) = \gamma_{dc}/\Gamma_{pd}(f)$ and ν is the waterfilling level that is selected to verify $\int_0^W \max\{0, 1/\nu - \alpha(f)\} df = W$. Key point here is to identify the magnitude of this gain when using commercial LEDs.

4. SIMULATION RESULTS

The office room size is $3\text{ m} \times 3\text{ m} \times 2.5\text{ m}$. The LED floor lamp has a height of 1.6 m and points up. Similarly, the PD points up and takes random locations on top of a desk of height 0.85 m. The PC-LED has a total radiant power $P_{led} = 50\text{ W}$, a measured SPD given in Fig. 2, viewing angle $\theta_{max} = 60\text{ deg}$, and time constants $\tau_p = 0.5\text{ }\mu\text{s}$ and $\tau_b = 0.05\text{ }\mu\text{s}$ for the Y-Phosphor and B-Chip, respectively. Similarly, the measured reflectance of the ceiling $\rho_{ceil}(\lambda)$, transmittance of the optical filter $f_o(\lambda)$, and responsivity of the PD $R_{pd}(\lambda)$ are shown in Fig. 3. The gain of the TIA is $G_{tia} = 750\text{ V/A}$ and the power invested on the DC-level of the DCO-OFDM signal is $\gamma_{dc} = 13\text{ dB}$ larger than the power used for the data symbols.

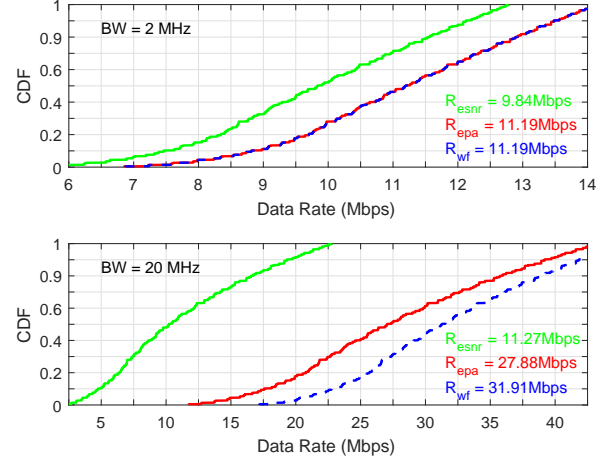


Fig. 5. CDF for the achievable data rate when DCO-OFDM bandwidth is 2 MHz (upper panel) and 20 MHz (lower panel). EPA: Solid red. ESNR: Solid green. WF: Dashed blue.

Figure 4 shows the CDF of the room illuminance, following the analysis presented in Section 3.1. Note that the mean illuminance requirements is verified since $E_{avg} = 515\text{ Lux}$, and the illuminance uniformity recommendation is also observed in most of the room area, as illuminance is only lower than 309 Lux in less than 8 % of the places (room corners).

Finally, Fig. 5 shows the CDF for the data rate when the bandwidth of the DCO-OFDM signal is $W = 2\text{ MHz}$ (upper panel) and $W = 20\text{ MHz}$ (lower panel). Since the frequency response of the PC-LED is almost flat at low frequencies (*i.e.*, Y-Phosphor emission range), no notable effects are observed when comparing EPA and WF for $W = 2\text{ MHz}$. On the contrary, since the variability of the PC-LED frequency response strengthens when the bandwidth of the DCO-OFDM signal grows (while becoming simultaneously more power-limited), the gain of WF with respect to EPA is more notable when $W = 20\text{ MHz}$. Finally, it is possible to see that the ESNR approach is not convenient, as too much power is wasted in compensating the low-gain frequency response that PC-LEDs have on the subcarriers with higher indexes.

5. CONCLUSION

We have studied the data rate that a DCO-OFDM VLC system can achieve with different power allocation schemes in an indoor office environment with indirect illumination. To make a reliable estimation of the actual data rate, the SPD of a commercial PC-LED and the reflectance of a sample ceiling material have been measured. Moreover, an off-the-shelf optical filter and PD have been considered. Although the frequency range in which a PC-LEDs has a good response is relatively narrow, it was observed that much higher data rates are feasible if the bandwidth of the DCO-OFDM signal goes beyond the cutoff frequency of the Y-Phosphor. In this case, WF power allocation outperforms EPA as the VLC link becomes more frequency-selective and power-limited.

6. REFERENCES

- [1] D. Karunatilaka, F. Zafar, V. Kalavally, and R. Parthiban, "LED based indoor visible light communications: State of the art," *IEEE Commun. Surveys & Tutorials*, vol. 17, no. 3, pp. 1649–1678, 3Q 2015.
- [2] G. Stepniak, M. Schüppert, and C. Bunge, "Advanced modulation formats in phosphorous LED VLC links and the impact of blue filtering," *J. Lightwave Tech.*, vol. 33, no. 21, pp. 4413–4423, Nov. 2015.
- [3] H. Elgala, R. Mesleh, and H. Haas, "Indoor broadcasting via white LEDs and OFDM," *IEEE Trans. Consumer Electronics*, vol. 55, no. 3, pp. 1127–1134, Aug. 2009.
- [4] H. Elgala, R. Mesleh, and H. Haas, "Indoor optical wireless communication: potential and state-of-the-art," *IEEE Commun. Mag.*, vol. 49, no. 9, pp. 56–62, Sept. 2011.
- [5] Z. Zhu, X. Jin, H. Yang, and L. Zhong, "Design of diffuse reflection freeform surface for uniform illumination," *J. Display Tech.*, vol. 10, no. 1, pp. 7–12, Jan. 2014.
- [6] Z. Lu, P. Tian, H. Fu, et al., "Experimental demonstration of non-line-of-sight visible light communication with different reflecting materials using a GaN-based micro-LED and modified IEEE 802.11 ac," *AIP Advances*, vol. 8, no. 10, pp. 1–9, Oct. 2018.
- [7] N. Hassan, Z. Ghassemlooy, S. Zvanovec, P. Luo, and H. Le-Minh, "Non-line-of-sight $2 \times N$ indoor optical camera communications," *Appl. Opt.*, vol. 57, no. 7, pp. B144–B149, Mar. 2018.
- [8] J. Armstrong, "OFDM for optical communications," *J. Lightwave Tech.*, vol. 27, no. 3, pp. 189–204, Feb. 2009.
- [9] A. Dowhuszko and A. Pérez-Neira, "Achievable data rate of coordinated multi-point transmission for visible light communications," in *Proc. Int. Symp. Personal, Indoor and Mobile Radio Commun.*, Oct. 2017, pp. 1–7.
- [10] B. Genovés Guzmán, A. Dowhuszko, V. Gil Jiménez, and A. Pérez-Neira, "Robust cooperative multicarrier transmission scheme for optical wireless cellular networks," *IEEE Photonics Technology Letters*, vol. 30, no. 2, pp. 197–200, Jan. 2018.
- [11] Lumileds, "LUXEON Rebel PLUS — The original high power LED," July 2017, DS107 LUXEON Rebel PLUS Product Datasheet, url: <https://www.lumileds.com/uploads/380/DS107-pdf>.
- [12] R. Zheng, "Luminous efficiency and color rendering of phosphor-converted white LEDs," *J. Light and Visual Environment*, vol. 32, no. 2, pp. 180–183, Feb. 2008.
- [13] K. Lee, H. Park, and J. Barry, "Indoor channel characteristics for visible light communications," *IEEE Commun. Letters*, vol. 15, no. 2, pp. 217–219, Feb. 2011.
- [14] Thorlabs, "PDA100A2 Si switchable gain detector — User guide," May 2019, url: <https://www.thorlabs.com/>.
- [15] Thorlabs, "FGS900 – Ø25 mm KG3 colored glass bandpass filter, 315-710 nm," Aug. 2011, url: <https://www.thorlabs.com/>.
- [16] T. Komine and M. Nakagawa, "Fundamental analysis for visible-light communication system using LED lights," *IEEE Trans. Consumer Electronics*, vol. 50, no. 1, pp. 100–107, Feb. 2004.
- [17] NSAI, "Light and lighting — Lighting of work places — Part 1: Indoor work places," June 2011, Irish Standard I.S. EN 12464.